

Low-Temperature Resistivity Anomalies in Periodic Curved Surfaces

Shota Ono and Hiroyuki Shima

Department of Applied Physics, Graduate School of Engineering, Hokkaido University, Sapporo 060-8628, Japan

arXiv:0909.1135v1 [cond-mat.mes-hall] 7 Sep 2009

Abstract

Effects of periodic curvature on the the electrical resistivity of corrugated semiconductor films are theoretically considered. The presence of a curvature-induced potential affects the motion of electrons confined to the thin curved film, resulting in a significant resistivity enhancement at specific values of two geometric parameters: the amplitude and period of the surface corrugation. The maximal values of the two parameters in order to observe the corrugation-induced resistivity enhancement in actual experiments are quantified by employing existing material constants.

Key words: surface curvature, electron-electron umklapp scattering, low-temperature resistivity

1. Introduction

Geometric curvature of nano-scale conducting films with curved geometry[1, 2, 3] provides us a clue to synthesize a new class of quantum devices based on curved nanomaterials. The most relevant nature is the occurrence of a *curvature-dependent potential* (CP) that acts on low-energy electrons moving in the curved systems[4, 5, 6, 7, 8]. The mechanism of the CP have been considered from various perspectives[9, 10, 11, 12, 13, 14, 15, 16], which triggered interesting theoretical predictions on the electric transport properties of curved nanostructures: quantum transmission probabilities in Y-nanojunction[17], a charge separation in helicoidal ribbons[18], and an anomalous shift of the Tomonaga-Luttinger exponent in deformed nanocylinders[19, 20] are only a few to mention.

In the earlier work, the authors have studied the CP effect on the electrical resistivity of corrugated semiconductor films[21]. A specific magnitude of the corrugation amplitude turned out to cause a significant increase in the resistivity, which is due to the CP-enhanced population of the electron-electron umklapp scattering processes relevant to the resistivity. This result motivates us to complete a thorough check of the CP effect in a wider range of two geometric parameters, i.e., the corrugation amplitude and period, that determine the shape of the corrugated film. This attempt is crucially important in order to make use of the effect in developing curved-nanomaterial-based quantum devices.

In this paper, we analyze systematically the correlation between the two geometric parameters and the CP-induced resistivity enhancement of the corrugated semiconductor films. We show that the degree of contributions from electron-electron scatterings to the resistivity is strongly dependent on the values of the two parameters. The present results enable to determine the maximal surface geometry that is requisite for the resistivity enhancement to get sizable in actual experiments.

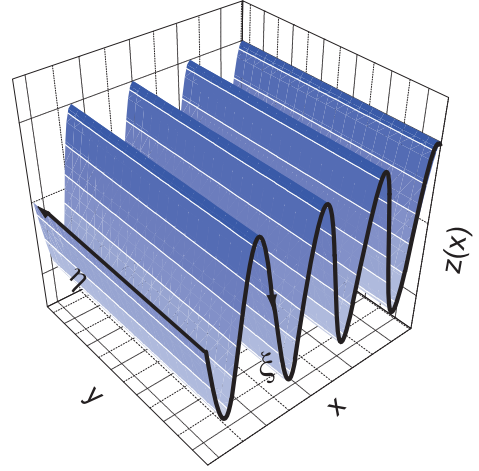


Figure 1: Sketch of a periodic curved surface. It is represented by $z = a \cos(\gamma x)$ with a corrugation amplitude a and a period $2\pi/\gamma$. The curvilinear coordinates (ξ, η) used in this paper are embedded in the surface.

2. Gap formation by periodic curvature

Let us consider a two dimensional (2D) electron system confined to a thin film, in which the film is subjected to an unidirectional corrugation along the x axis. The height of the film in the z direction is given by

$$z = a \cos(\gamma x), \quad (1)$$

where a and $2\pi/\gamma$ are the amplitude and period of corrugation, respectively (see Fig. 1). By transforming the variables x, y into

$$\xi = \int_0^x w(x') dx', \quad \eta = y, \quad (2)$$

with the definition $w(x) = \sqrt{1 + (\partial z / \partial x)^2}$, we obtain the Schrödinger equation [21]

$$\left[-\frac{\hbar^2}{2m^*} \left(\frac{\partial^2}{\partial \xi^2} + \frac{\partial^2}{\partial \eta^2} \right) + U(\xi) \right] \psi(\xi, \eta) = E \psi(\xi, \eta). \quad (3)$$

Here, the potential $U(\xi)$ is the CP associated with the periodic corrugation,

$$U(\xi) = -\frac{\hbar^2}{8m^*} \frac{[a\gamma^2 \cos(\gamma x)]^2}{\{1 + [a\gamma \sin(\gamma x)]^2\}^3}, \quad (4)$$

and m^* is the effective mass of conducting electrons. Equation (3) is solved by using the Fourier series expansion

$$\psi(\xi, \eta) = \left[\sum_{k_\xi} \alpha_{k_\xi} \exp(ik_\xi \xi) \right] \exp(ik_\eta \eta), \quad (5)$$

as a result of which the energy-band structure $E = E(\mathbf{k})$ with respect to the wavevector $\mathbf{k} = (k^\xi, k^\eta)$ is obtained.

The periodic nature of $U(\xi)$ with the period $\Lambda_\xi = \int_0^{\pi/\gamma} w(x)dx$ implies an occurrence of gaps at $k^\xi = \pm nG^0/2$ (n is a positive integer) in the Fermi circle, where $G^0 \equiv 2\pi/\Lambda_\xi$ defines the reciprocal lattice vector $\mathbf{G} \equiv (G^0, 0)$ associated with the periodicity of $U(\xi)$. Such gaps are observed in Fig. 2(b), where a sufficiently large amplitude of $U(\xi)$ is assumed by setting appropriate values of a and γ . Still, it should be noted that gaps at $k^\xi = \pm nG^0/2$ may and may not occur once G^0 is given. This is primary because G^0 as well as Λ_ξ are two-variable functions of a and γ as understood from Fig. 1. Hence, different pairs of the two values $\{a, \gamma\}$ can yield the same value of G^0 , though the pairs do not always produce a gap at $k^\xi = \pm nG^0/2$.

Two contrast examples of the Fermi circle are clearly demonstrated in Figs. 2(a) and 2(b). We set $\{k_F a, \lambda_F \gamma\} = \{0.7, 3.1\}$ and $\{2.7, 7.1\}$ to draw the Fermi circles, in which both pairs give an identical value of G^0 as shown in the contour plot of $G^0/(2k_F)$ in Fig. 3; the points **A** and **B** in the plot correspond to Fig. 2(a) and 2(b), respectively. The Fermi circle in Fig.2(a) has almost no gap, whereas that in Fig.2(b) shows clear gaps at $k^\xi/k_F = \pm G^0/(2k_F)$ and $\pm G^0/k_F$. As we shall see later, usage of such pairs $\{a, \gamma\}$ that lead to gaps in the Fermi circle is a necessary condition for the corrugation-induced jump in the resistivity to be observed.

3. Resistivity of the corrugated film

We now consider the low-temperature resistivity of 2D electron systems under periodic modulation. Contributions of two-electron scatterings to the resistivity at low temperature T are expressed by [21, 22]

$$\rho(T) = \rho_c \left(\frac{k_B T}{E_F} \right)^2 \frac{h}{e^2}, \quad \rho_c = \sum_{n=-\infty}^{\infty} C(n), \quad (6)$$

where k_B, E_F are the Boltzmann constant and the Fermi energy, respectively. $C(n)$ represent the contributions from the n th umklapp scatterings $(\mathbf{k}_1, \mathbf{k}_2) \rightarrow (\mathbf{k}_3, \mathbf{k}_4)$ that satisfy the momentum conservation law:

$$\mathbf{k}_3 + \mathbf{k}_4 = \mathbf{k}_1 + \mathbf{k}_2 + n\mathbf{G}. \quad (7)$$

$C(n) = C(-n)$ is satisfied because of the inversion symmetry of the Fermi circle with respect to $k^\xi = 0$. Equation (6) holds for $k_B T \ll E_F$, i.e., when smearing of the Fermi degeneracy by

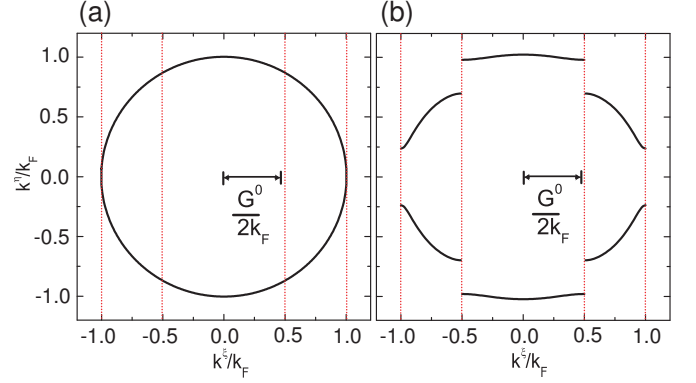


Figure 2: Fermi circles of the corrugated system with: (a) $\{k_F a, \lambda_F \gamma\} = \{0.7, 3.1\}$, and (b) $\{k_F a, \lambda_F \gamma\} = \{2.7, 7.1\}$. Gaps open at $k^\xi/k_F = \pm G^0/(2k_F)$ and $\pm G^0/k_F$ only in Fig. 2(b).

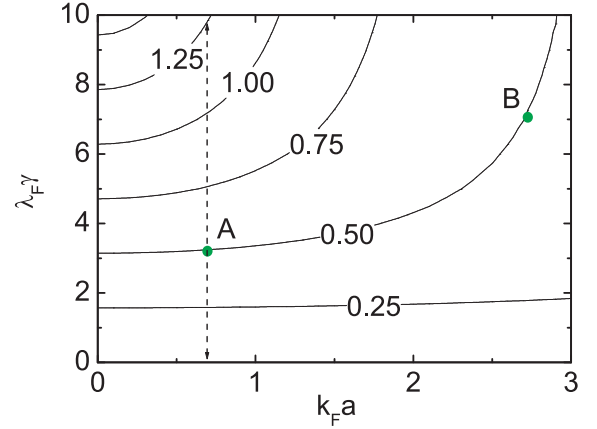


Figure 3: Contour plot of $G^0/(2k_F)$ as a function of a and γ . The points **A** and **B** indicate the numerical conditions to deduce the gapped (or no-gapped) Fermi circle depicted in Figs. 2(a) and 2(b), respectively

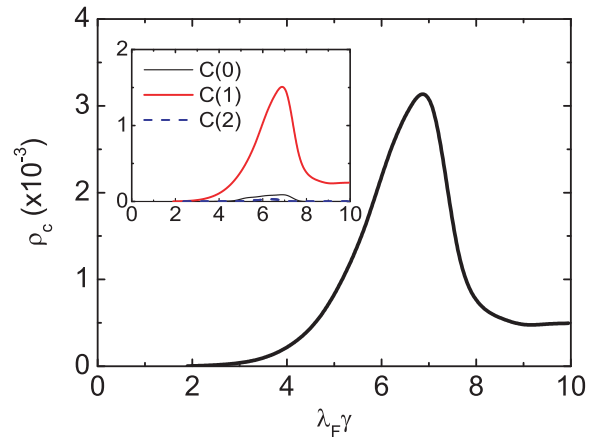


Figure 4: Resistivity coefficient ρ_c as a function of γ with $k_F a = 0.7$. ρ_c shows the maximum at $\lambda_F \gamma = 7.0$. Inset: n th-order contributions $C(n)$ for $n = 0, 1, 2$. The first umklapp process plays a dominant role in determining ρ_c .

thermal fluctuation can be negligible so that electron-electron scatterings are allowed just on the Fermi circle.

Each $C(n)$ in Eq. (6) sums up contributions from all possible n th-order processes $(\mathbf{k}_1, \mathbf{k}_2) \rightarrow (\mathbf{k}_3, \mathbf{k}_4)$ that satisfy Eq. (7). Among many processes, specific ones involving the state \mathbf{k} that locates near the gap are dominant in the total value of $C(n)$ [21]. Furthermore, the number of such dominant processes takes the maximum when gaps open at both ends of the Fermi circle ($k^\xi = \pm k_F$), i.e., when the relation

$$\frac{G^0}{2k_F} = \frac{1}{n} \quad (n = 1, 2, \dots), \quad (8)$$

is satisfied. As a result, the surface corrugation with a and γ that satisfy Eq. (8) can cause the corrugation-induced jump in ρ_c . We emphasize again that Eq. (8) is a necessary (not sufficient) condition of the jump in ρ_c , since gaps may and may not be present for a given G^0 .

4. Numerical Results

In numerical calculations of ρ_c , we set $E_F = 10\text{meV}$ and employed material constants of the GaAs/Al_xGa_{1-x}As heterostructures: the effective mass is $m^*/m_0=0.067$ (m_0 is a bare electron mass) and the dielectric constant is $\epsilon/\epsilon_0=13.2$ (ϵ_0 is the dielectric constant of vacuum).

Figure 4 shows the γ dependence of ρ_c ; we fixed $k_F a=0.7$ and increased γ from $\lambda_F \gamma = 0$ to $\lambda_F \gamma = 10$ as indicated by the dotted trajectory in Fig. 3. ρ_c has a peak at $\lambda_F \gamma = 7.0$ under the condition of $k_F a = 0.7$, which is a consequence of the satisfied relation $G^0/(2k_F) = 1$ as seen from Fig. 3. Hence, the peak of ρ_c at $\lambda_F \gamma = 7.0$ tells us that the pair $\{a, \gamma\}$ of the above mentioned values generates gaps at $k^\xi = \pm k_F$ in the Fermi circle. In the inset of Fig. 4, we also show the γ dependences of $C(n)$ with $n = 0, 1$ and 2 . The term $C(1)$ is found to be dominant at all values of $\lambda_F \gamma$, which imply that overall behavior of ρ_c in the γ region considered is determined by the first-order umklapp process.

It should be noted that in Fig. 4, no peak appears at $\lambda_F \gamma = 3.1$ although the value satisfies the condition of Eq. (8) with $n = 2$. The disappearance of the peak in ρ_c at $\lambda_F \gamma = 3.1$ is attributed to the absence of gaps associated with the second-order umklapp process, as discussed below in detail.

5. Discussions

We discuss the reason why the contributions from the second umklapp processes do not enhance ρ_c at $\lambda_F \gamma = 3.1$ in Fig. 4. Figures 5(a) and 5(b) show the profiles of the Fourier coefficients $|\alpha_{k^\xi}|$ (see Eq. (5)) under the numerical conditions of **A** and **B** marked in Fig. 3, respectively. In both figures, upward peaks of $|\alpha_{k^\xi \pm nG^0}|$ with $n \neq 0$ touch downward peaks of $|\alpha_{k^\xi}|$ at $k^\xi/k_F = \mp nG^0/(2k_F)$. The widths $\Delta k^\xi(n)$ of the upward peaks are estimated as [23]

$$\frac{\Delta k^\xi(n)}{k_F} = \frac{k_F}{nG^0} \frac{|U_{nG^0}|}{E_F}, \quad (9)$$

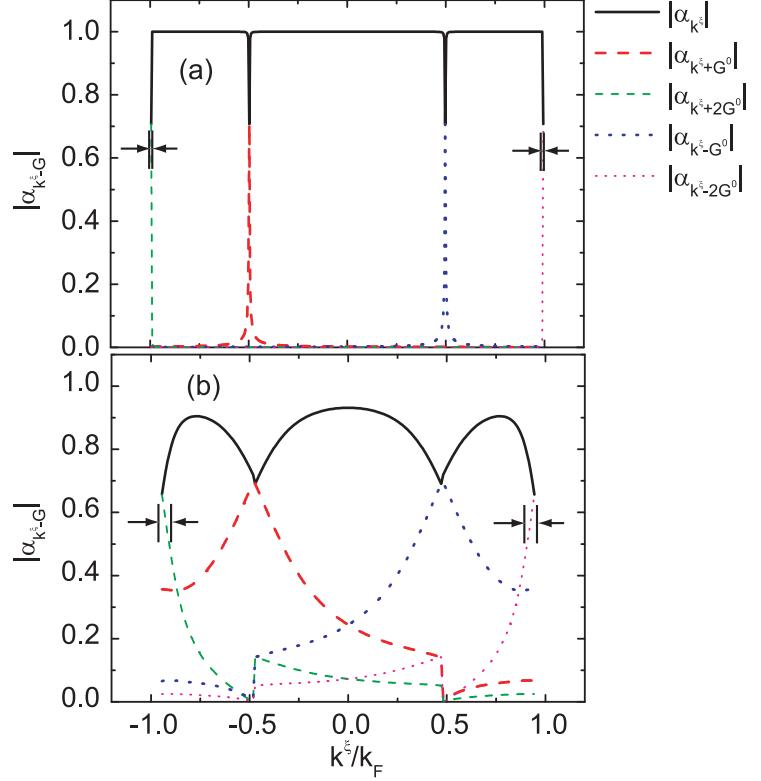


Figure 5: Profile of the Fourier coefficients $|\alpha_{k^\xi}|$ defined by Eq. (5) as a function of k^ξ . Plots in (a) and (b) correspond to $\{k_F a, \lambda_F \gamma\} = \{0.7, 3.1\}$ and $\{2.7, 7.1\}$, respectively. The width of the upward peaks $\Delta k^\xi(n)/k_F$ for $n = 2$ are signified by arrows.

where U_{nG^0} is the Fourier component of the CP. We can deduce from Eq. (9) that $\Delta k^\xi(2)/k_F \sim 10^{-5}$ for **A** and $\sim 10^{-1}$ for **B**; furthermore, it follows from Eq. (9) that $\Delta k^\xi(n)/k_F$ increases monotonically with increasing a and γ . Notice that the larger width $\Delta k^\xi(n)/k_F$ results in the larger ρ_c , since the number of the associated umklapp processes increase. In fact, $\Delta k^\xi(n)/k_F \geq 10^{-2}$ is needed to get $\rho_c \geq 10^{-3}$ under the condition that $\{k_F a, \lambda_F \gamma\}$ yields $G^0/(2k_F) = 1$ or 2 . (The magnitude of $\rho_c \sim 10^{-3}$ is large enough to observe it experimentally[24].) These arguments account for the reason why the parameters $\{a, \gamma\}$ corresponding to **A**, which provide $\Delta k^\xi(2)/k_F \sim 10^{-5} \ll 10^{-2}$, give no peak in ρ_c in Fig. 4.

We have also confirmed that $k_F a \geq 0.5$ for $n = 1$ and $k_F a \geq 2.0$ for $n = 2$ are enough to yield $\Delta k^\xi(n)/k_F \geq 10^{-2}$, where $0 < \lambda_F \gamma < 10$ is assumed. Our results reveal the geometric conditions of the surface corrugation to obtain a sizable jump in ρ_c of a semiconductor film. The same approach is applicable to other semiconducting materials than the GaAs/Al_xGa_{1-x}As heterostructures we have considered.

6. Conclusion

In conclusion, we have demonstrated the curvature-induced enhancement of ρ_c of periodically curved thin films at low T . Appropriate values of a and γ for the resistivity enhancement to appear in measurements have been clarified using existing

material constants. The umklapp contributions to the resistivity have been found to increase significantly when the value of a and γ satisfy the conditions given by $G^0/(2k_F) = 1/n$ and $\Delta k^\xi(n)/k_F \geq 10^{-2}$. We hope that experimental tests of our theoretical predictions open a gate for next-generation devices based on curved nanostructures.

Acknowledgments

We would like to thank K. Yakubo, S. Nishino, H. Suzuura, and S. Uryu for useful discussions and suggestions. This study was supported by a Grant-in-Aid for Scientific Research from the MEXT, Japan. H.S. is thankful for the financial support from Executive Office of Research Strategy in Hokkaido University. A part of numerical simulations were carried out using the facilities of the Supercomputer Center, ISSP, University of Tokyo.

References

- [1] V. Ya. Prinz, D. Grützmacher, A. Beyer, C. David, B. Ketterer and E. Deckardt, *Nanotechnology* **12**, 399 (2001).
- [2] A. Lorke, S. Bohm and W. Wegscheider, *Superlattices Microstruct.* **33**, 347 (2003).
- [3] V. Ya. Prinz, *Phys. Status. Solidi B* **243**, 3333 (2006).
- [4] H. Jensen and H. Koppe, *Ann. Phys.* **63**, 586 (1971).
- [5] R. C. T. da Costa, *Phys. Rev. A* **23**, 1982 (1981).
- [6] M. Ikegami and Y. Nagaoka, *Prog. Theor. Phys.* **106**, 253 (1991).
- [7] L. Kaplan, N. T. Maitra and E. J. Heller, *Phys. Rev. A* **56**, 2592 (1997).
- [8] P. C. Schuster and R. L. Jaffe, *Ann. Phys.* **307**, 132 (2003).
- [9] G. Cantele, D. Ninno and G. Iadonisi, *Phys. Rev. B* **61**, 13730 (2000).
- [10] M. V. Entin and L.I. Magarill, *Phys. Rev. B* **64**, 085330 (2001).
- [11] H. Aoki, M. Koshino, D. Takeda, and H. Morise, *Rhys. Rev. B* **65**, 035102 (2001).
- [12] N. Fujita, *J. Phys. Soc. Jpn.* **73**, 3115 (2004).
- [13] J. Gravesen and M. Willatzen, *Phys. Rev. A* **72**, 032108 (2005).
- [14] A. Marchi, S. Reggiani, M. Rudan and A. Bertoni, *Phys. Rev. B* **72**, 035403 (2005).
- [15] M. Encinosa, *Phys. Rev. A* **73**, 012102 (2006).
- [16] G. Ferrari and G. Cuoghi, *Phys. Rev. Lett.* **100**, 230403 (2008).
- [17] G. Cuoghi, G. Ferrari and A. Bertoni, *Phys. Rev. B* **79**, 073410 (2009).
- [18] V. Atanasov and R. Dandolo and A. Saxena, *Phys. Rev. B* **79**, 033404 (2009).
- [19] H. Shima, H. Yoshioka, and J. Onoe, *Phys. Rev. B* **79**, 201401(R) (2009).
- [20] H. Shima, H. Yoshioka, and J. Onoe, arXiv: 0908.2565.
- [21] S. Ono and H. Shima, *Phys. Rev. B* **79**, 235407 (2009).
- [22] S. Uryu and T. Ando, *Phys. Rev. B* **64**, 195334 (2001).
- [23] C. Kittel, *Introduction to Solid State Physics* (John Wiley and Sons, Inc., New York, Seventh Edition, 1996).
- [24] A. Messica, A. Soibel, U. Meirav, A. Stern, H. Shtrikman, V. Umansky, and D. Mahalu, *Phys. Rev. Lett* **78**, 705 (1997).